

# Soft-Contact Optical Lithography Using Transparent Elastomeric Stamps: Application to Nanopatterned Organic Light-Emitting Devices

By Tae-Woo Lee,\* Seokwoo Jeon, Joana Maria, Jana Zaumseil, Julia W. P. Hsu, and John A. Rogers\*

Conventional photolithography uses rigid photomasks of fused quartz and high-purity silica glass plates covered with patterned microstructures of an opaque material. We introduce new, transparent, elastomeric molds (or stamps) of poly(dimethylsiloxane) (PDMS) that can be employed as photomasks to produce the same resist pattern as the pattern of the recessed (or non-contact) regions of the stamps, in contrast to other reports in the literature<sup>[1]</sup> of using PDMS masks to generate edge patterns. The exposure dose of the non-contact regions with the photoresist through the PDMS is lower than that of the contact regions. Therefore, we employ a difference in the effective exposure dose between the contact and the non-contact regions through the PDMS stamp to generate the same pattern as the PDMS photomask. The photomasking capability of the PDMS stamps, which is similar to rigid photomasks in conventional photolithography, widens the application boundaries of soft-contact optical lithography and makes the photolithography process and equipment very simple. This soft-contact optical lithography process can be widely used to perform photolithography on flexible substrates, avoiding metal or resist cracks, as it uses soft, conformable, intimate contact with the photoresist without any external pressure. To this end, we demonstrate soft-contact optical lithography on a gold-coated PDMS substrate and utilized the patterned Au/PDMS substrate with feature sizes into the nanometer regime as a top electrode in organic light-emitting diodes that are formed by soft-contact lamination.

## 1. Introduction

Conventional photolithography usually uses photomasks of rigid, fused quartz and high-purity silica glass plates covered with patterned microstructures of an opaque material such as chrome. In this conventional process, a vacuum and pressure are necessary to enhance the resolving power by reducing the air gap between the photomask and the photoresist, but intimate contact between them is still difficult because of the rigidity of the photomasks.

Herein, we report a form of soft-contact optical lithography using a transparent elastomer, poly(dimethylsiloxane) (PDMS) as an optical mask. High-resolution pattern-transfer elements made of PDMS have been employed in various soft-lithographic techniques,<sup>[2]</sup> such as microcontact printing,<sup>[2]</sup> micromolding in capillaries,<sup>[2]</sup> and nanotransfer printing.<sup>[3]</sup> These are low-cost, large-area tools that have promising potential applications in the area of flexible plastic optoelectronic systems. This photo-

lithographic approach of using transparent PDMS stamps—formed using the established techniques of soft lithography—as optical masks to pattern structures of photoresist on rigid or flexible substrates enables intimate contact between the stamp and the photoresist, owing to van der Waals' interactions. Although phase-shift edge lithography using PDMS stamps has been reported,<sup>[1,4,5]</sup> the application is limited to obtaining only edge patterns. However, we have found that, using the same PDMS stamps, we can obtain the same resist pattern as the recessed (or non-contact) regions of the PDMS stamps as we do in conventional photolithography. We utilized the relative difference in the effective exposure dose between the contact and the non-contact regions through the PDMS stamp to generate the same pattern as the non-contact regions of the PDMS photomask. The photomasking capability of the PDMS stamps, which is similar to that of rigid photomasks in conventional photolithography, in addition to generating the edge-pattern, enlarges the application boundaries of soft-contact optical lithography.

Herein, we show that this soft-contact optical lithography results in two different patterns, depending on the exposure and developing conditions. Full-vector finite-element modeling of Maxwell's equations reveals the optics of this form of photolithography: This process can be widely used to perform photolithography on rigid (e.g., silicon wafer, glass) or flexible (e.g., PDMS, poly(ethylene terephthalate) or other plastics) substrates at a low cost. In addition, it can be particularly useful for avoiding metal or resist cracks on the flexible substrate. In this respect, we first demonstrate soft-contact optical lithography on a gold-coated PDMS substrate. While microcontact printing using PDMS stamps has been used successfully for

[\*] Dr. T.-W. Lee, J. Zaumseil, Dr. J. W. P. Hsu  
Bell Laboratories, Lucent Technologies  
600 Mountain Avenue, Murray Hill, NJ 07974 (USA)  
E-mail: taew.lee@samsung.com  
Prof. J. A. Rogers, S. Jeon, J. Maria  
Department of Materials Science and Engineering  
Department of Chemistry, Beckman Institute  
and Seitz Materials Research Laboratory  
University of Illinois at Urbana-Champaign  
Urbana, IL 61801 (USA)  
E-mail: jarogers@uiuc.edu

patterning metal electrodes on flexible substrates,<sup>[6–8]</sup> photolithography using rigid photomasks can induce metal or photoresist cracks on the surface. However, this soft-contact photolithography enables the metal to be patterned on the flexible substrate via regular photolithography. After this photolithography, selective etching of a preformed uniform layer of gold on the PDMS using the patterned resist as an etch mask yields metal patterns with the geometry of the resist pattern. These can be used as electrodes in various electronic or optoelectronic devices. We show utilization of a patterned Au/PDMS substrate with nanoscale feature sizes as a top electrode in organic light-emitting diodes (OLEDs). Soft-contact lamination<sup>[6–8]</sup> of the resulting patterned electrode structures against an electroluminescent polymer yields working OLEDs with emission areas with dimensions of  $\approx 150$  nm and  $\approx 800$  nm. Owing to the flexibility of the electrode geometries that are possible with this approach, and its ability to allow patterning of the top electrode in OLED structures, it forms a useful complement to other recently described methods for building nanoscale OLEDs.<sup>[9]</sup>

## 2. Results and Discussion

Figure 1 shows a schematic diagram of the use of PDMS masks for optical lithography on Au/Ti/PDMS. A prepolymer of PDMS (Dow corning, Sylgard 184) was cast and cured (3 h at 60 °C) against a flat and clean silicon wafer surface. Mounting this flat PDMS ( $\approx 4$  mm thick) element against a glass slide and then exposing it to an oxygen plasma for about 2 s (30 sccm, 30 mT, 100 V; Plasma-Therm reactive-ion etcher), followed by electron-beam evaporation of a bilayer of titanium (1 nm, 0.3 nm/s, adhesion promoter)/gold (20 nm, 1 nm/s) generated smooth, crack-free metal films strongly bonded to the PDMS.<sup>[10]</sup> Spin-casting photoresist (Shipley 1805) onto this Au/Ti/PDMS element at 4000 rpm for 10 s formed a coating with a thickness of  $\approx 400$  nm. To avoid inducing cracks in the gold, we did not bake the photoresist after spinning; it was left in air for  $\approx 5$  min.

Casting and curing the same PDMS prepolymer against photolithographically patterned lines of photoresist (Shipley 1805, 4000 rpm spin speed) on a silicon wafer formed a conformable PDMS optical mask (relief  $\approx 400$  nm; thickness  $\approx 4$  mm) that was transparent to visible and UV light. The relief depth ( $\approx 400$  nm) of the photomask shifted the phase of the transmitted UV light by an amount close to  $\pi$ .<sup>[4]</sup> Contacting this mask with the photoresist/Au/PDMS substrate, exposing the structure to collimated UV light (filtered to generated light with a wavelength centered at 330 nm; intensity  $\approx 240 \mu\text{W cm}^{-2}$ ), removing the mask, developing the resist and, finally, etching the underlying gold (Transene GE 8148;  $\approx 3$  s) and removing the resist, completed the process. By controlling the exposure and developing conditions we could, using a single PDMS mask, generate patterns with characteristic dimensions of a few micrometers (Process I: left route in Fig. 1) down to  $\approx 150$  nm (Process II: right route in Fig. 1). We regulated the exposure dose by changing the exposure time. The exposure dose of the non-contact region

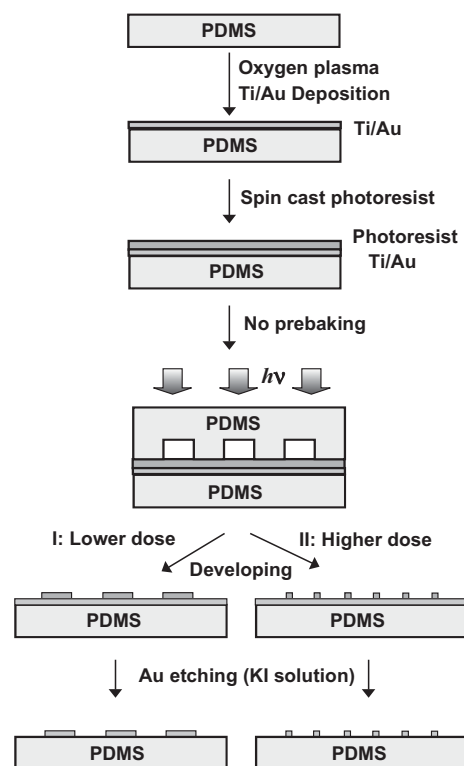


**Figure 1.** Schematic illustration of the soft-contact optical lithography process using PDMS in the near-field, with a conformal elastomeric optical or phase mask. Flat cured PDMS ( $\approx 4$  mm) was prepared on a clean silicon wafer supported by a glass slide; it was then exposed to oxygen plasma for about two seconds. Titanium (1 nm)/gold (20 nm) was deposited on the PDMS using an electron-beam evaporator at  $\approx 5 \times 10^{-7}$  torr (1 torr  $\approx 133$  Pa) to generate thin, electrically continuous metal films that were strongly bonded to the PDMS. Photoresist (Shipley 1805, positive) was spin-cast on the Au/PDMS at 4000 rpm for 10 s. To avoid cracking the gold, we did not bake the film after spinning. An optical mask (relief:  $\approx 400$  nm; thickness:  $\approx 4$  mm), which was transparent to visible and UV light, was laminated on the top of the photoresist. The resist was then exposed to collimated UV light passing through the PDMS mask and was developed. We controlled the exposure dose to obtain different line-width patterns. With lower exposure doses, we duplicated the PDMS relief pattern; at higher exposure doses, we obtained line widths from 50 to 150 nm by phase-shifts in the optical near-field.

(with the photoresist through the PDMS) was lower than that of the contact region (Fig. 2b). Therefore, we employed the difference in effective exposure dose between the contact and the non-contact regions through the PDMS mask to generate two types of patterns (Process I or Process II). When the effective exposure dose through the non-contact region of the PDMS was insufficient for the non-contact part to be removed after development in a moderate developing solution (a 3:2 mixture of Shipley 452 with water) for a given developing time (50 s), but the exposure dose through the contact region was still enough for the contact region of the photoresist to be removed after development, we could obtain patterns similar to those obtained by conventional photolithography using a rigid glass or quartz photomask (Process I). On the other hand, with higher exposure dose under the same developing conditions (i.e., with the same developer and for the same developing time) or with the same

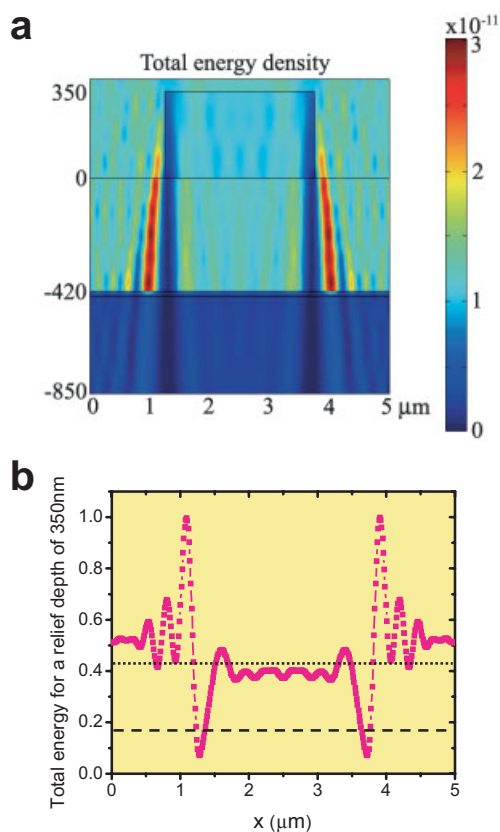


**Figure 2.** Simulation plot of near-field surface intensity passing through a PDMS phase mask whose refractive index is 1.467. The wavelength in this simulation is 315 nm. The relief depth of the mask is 350 nm, which is not far from  $\pi$ -shift conditions. A contour plot of total energy distribution in space (a) visualizes the propagation of energy. A line cut at a depth of 10 nm from the surface of the photoresist (b) shows that the average intensity is about 30% less than the raised mask region, where the PDMS is in direct contact with photoresist. The recessed line width is 2.5  $\mu\text{m}$ , and the periodicity is 5  $\mu\text{m}$ . The dotted (upper) line and the dashed (lower) line indicate the cut-off exposure doses for processes I,II of Fig. 1, respectively.

exposure dose as used in Process I, but for a much longer developing time, we could produce narrow ( $\approx 150$  nm) lines at the positions of the relief step edges on the PDMS mask (Process II). This type of patterning capability has been described previously.<sup>[1,4,5]</sup> We believe that this broad line-patterning capability is provided by the combined effects of differential effective exposure in the raised and recessed regions and a nonlinear response of the resist (which is derived from exposure-induced changes in the refractive index and absorption of the resist)<sup>[11]</sup> that is emphasized when exposure doses above the threshold are employed.

Figure 2 shows results from finite-element modeling of the intensity of light passing through a PDMS phase mask in contact with a photoresist/Au/PDMS substrate. The narrow dips in intensity at the edges of the relief, which are responsible for patterning the 150 nm line, are clearly visible (also see the dashed line in Fig. 2b). There is also, for certain wavelengths and depths of mask relief, a slight difference in the average in-

tensity in the recessed and raised regions (see the dotted line in Fig. 2b). It is possible that these slight differences can be amplified by the nonlinear response of the resist, giving rise to the broad line-patterning capability (Process I).<sup>[11]</sup> Further investigation of this phenomenon, which considerably expands the patterning flexibility afforded by the PDMS phase masks, is required. Herein, we simply report on the use of this capability to generate patterned emission from OLEDs formed by soft-contact lamination.

Figure 3 shows the gold patterns on PDMS obtained via processes I,II. Figures 3a,c illustrate the patterns in the geometry of the recessed regions of the masks (disks and lines) by using a high exposure dose and short developing time. Controlled over-etching of the gold during the fabrication of these structures could reduce their widths to about 0.8  $\mu\text{m}$ . Figures 3b,d

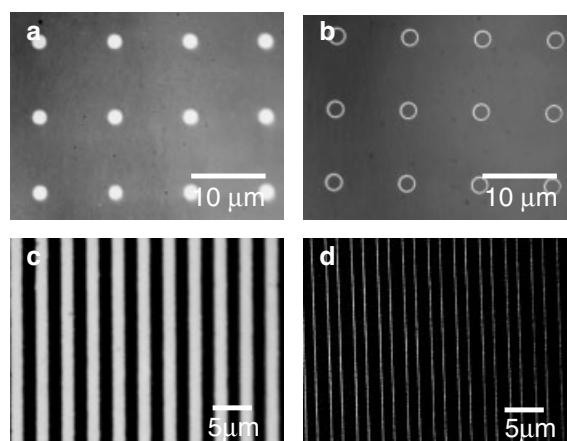


**Figure 3.** The patterned structures produced using soft-contact optical lithography with an elastomeric optical mask. Process I, which used the PMDS mask as a photomask to duplicate the PDMS pattern produces closed disk (a) and thick line (c) patterns; whereas process II, which used the PDMS mask as a phase-shift mask, gives open rings (b) and thin line (d) patterns with periodic spacing.

show narrow ( $\approx 150$  nm) line patterns (rings and lines, respectively) that form at the edges of the mask relief when sufficiently long developing times are used. The resulting gold patterns in both cases are electrically continuous. Some wrinkling of the surface of the bare PDMS after etching away the unprotected gold was sometimes observed.

Laminating these PDMS-supported patterned gold electrodes on 100 nm thick electroluminescent layers (a mixture of a polyfluorene derivative<sup>[12]</sup> and tetra-*n*-butylammonium tetrafluoroborate) spin-cast on indium tin oxide (ITO) glass, formed working OLEDs with emission patterns defined by the geometry of the electrodes. The left-hand images of Figures 4a,b show the electroluminescence (EL) patterns obtained from two devices. The nanopatterned OLEDs (Fig. 4b) have  $\approx 150$  nm wide gold line electrodes, but have emission profiles of  $\approx 600$  nm line width, which is comparable to the resolution of the optical imaging system (direct near-field inspection of the emission patterns was difficult because of the laminated construction).

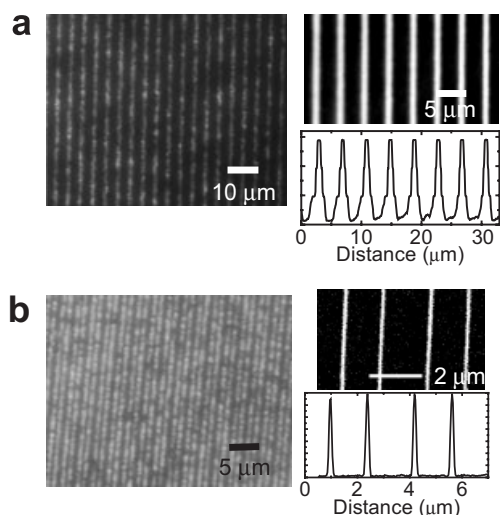


**Figure 4.** EL images of a soft-contact laminated device with gold lines/PDMS: a) 800 nm and b) 150 nm gold lines. The top right images in (a) and (b) show the patterned image of the gold lines/PDMS before lamination, while the bottom right graphs present the image-contrast profiles of the top right images, showing the resolution of the lines.

Figure 5 shows the current-density–voltage and luminescence characteristics of the nanopatterned OLEDs with  $\approx 150$  nm wide gold lines. The operating voltages are similar to those of microscale devices fabricated in a similar manner. The efficiency of the nanopatterned devices is a little lower (0.23 % with 20 nm gold) than that of the unpatterned ones (0.65 %). The EL spectrum of the nanopatterned device was quite similar to that of the unpatterned device (Fig. 5c, inset). This behavior is consistent with observations of nanoscale devices formed by nanosphere lithography.<sup>[10]</sup>

### 3. Conclusion

We have reported a soft-contact optical lithography process, which uses a PDMS stamp as an optical mask, and can result in two different patterns (the same pattern as the non-contact region of the PDMS stamp, and the edge pattern of the contact region of the PDMS stamp), depending on the exposure time and developing conditions. In particular, the photomasking capability of the PDMS stamps, which is similar to that of rigid photo-masks in conventional photolithography but has the added advantage of edge-pattern generation, widens the application boundaries of soft-contact optical lithography and makes the photolithography process and equipment very simple. Although this process can be used for photolithography on rigid substrates, it can also be widely employed for low-cost photolithography on flexible substrates. In this way, we can avoid metal cracks on the flexible substrates, as this process uses soft, conformable, and intimate contact with the photoresist without any external pressure. By combining soft-contact lamination with soft optical lithography for a patterned top electrode (Au/PDMS), we fabricated a patterned OLED with feature sizes in the nanometer regime: This is an easy way to perform top-electrode patterning

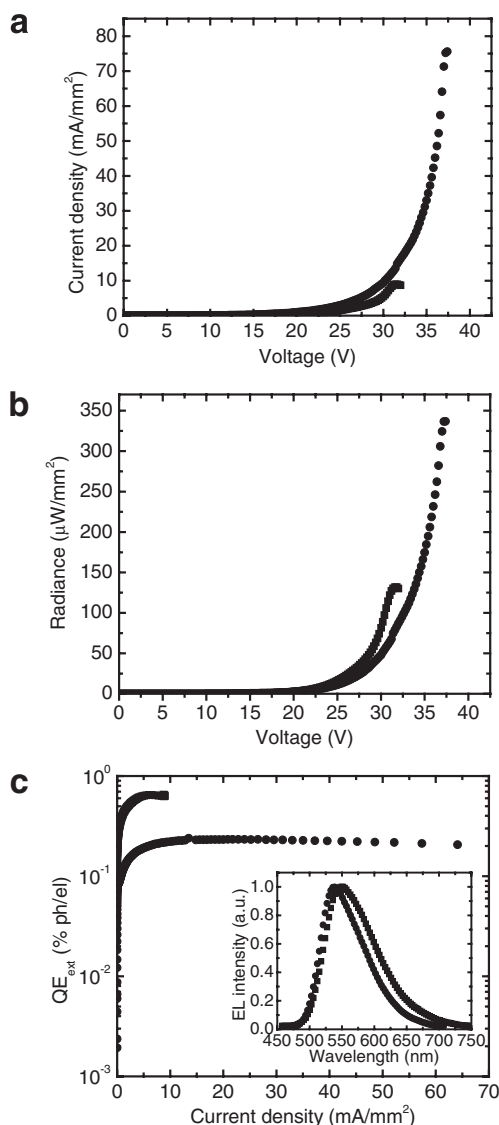


**Figure 5.** The current-density–voltage luminescence characteristics of the  $\approx 150$  nm nanopatterned OLEDs (●) compared with those of an unpatterned, soft-contact laminated device (■): a) current density versus voltage; b) radiance versus voltage; and c) external device quantum efficiency versus current density. The inset shows the electroluminescence spectra of the devices.

with high resolution, and could be a better way of achieving improved pattern resolution and quality than the conventional approach of modifying the bottom electrode.<sup>[13]</sup> Ultrasmall flexible OLEDs such as these could potentially be useful, for example, as conformable light sources for subwavelength storage or lithography systems, or nanoscale optoelectronics.

### 4. Experimental

A uniform film of the electroluminescent material (a mixture of a polyfluorene derivative and 17 wt.-% tetra-*n*-butylammonium tetrafluoroborate) was spin-cast on a thin ( $\approx 100$  nm) layer of ITO ( $\approx 15 \Omega$  square) on a glass slide (0.4 mm thick). When the bottom (ITO/emit-

ting layer) and top pieces (Au/PDMS) were brought together, van der Waals' forces pulled the electrodes into intimate contact with the EL layer at room temperature, without the application of external pressure. Typically, this contact was initiated on one side of the structure; a wetting front then progressed naturally across the sample, until the entire surface was in contact. In all cases, the metal-coated PDMS was either used to build devices immediately after evaporation, or after removal from brief storage in a dry nitrogen environment. We observed the complete lamination over the entire surface through a microscope after laminating the top electrode over the electroluminescent materials on an ITO glass substrate. Optical modeling was based on full-vector calculations of Maxwell's equation by the finite-element method (FEMLAB, the Mathworks, Inc.). Grating geometry was solved for the transverse electric (TE) ( $E_z, H_z=0$ ) mode using a linear solver included in the Electromagnetics Module. Boundary conditions (BC) for the TE Mode: low-reflecting BC on top and bottom of the line grating and PMC (perfect magnetic boundary conditions) on the sides of the grating were used to capture its "infinite size". The mesh elements in the photoresist were 7 and 50 nm everywhere else.

Two soft-contact laminated devices were made, one with 800 nm and the other with 150 nm gold lines. The 800 nm gold lines were prepared by over-etching the gold lines after Process I (Fig. 1). The 150 nm gold lines were prepared by Process II (Fig. 1). Contrast profiles of the devices were obtained by averaging line-cuts perpendicular to the pattern lines using the Spyglass Transform software. The gold was 20 nm thick and the electroluminescent layer was 100 nm thick. Photolithography with a conformable phase mask was followed by the direct etching of the pattern lines (150 nm wide) of gold on the PDMS. The average line width ( $\approx 600$  nm) of the pattern of emission (right bottom graph of Fig. 4b) in this case is comparable to the resolution of the optical imaging system. The Rayleigh diffraction limit for the 0.55 numerical aperture microscope objectives is 590 nm at a wavelength of 540 nm. The EL image was taken through the ITO (100 nm)/glass (0.4 mm), which reduces the effective numerical aperture.

Received: February 24, 2005

Final version: April 12, 2005

Published online: July 20, 2005

- [1] J. A. Rogers, K. E. Paul, R. J. Jackman, G. M. Whitesides, *Appl. Phys. Lett.* **1997**, *70*, 2658.
- [2] Y. Xia, G. M. Whitesides, *Angew. Chem. Int. Ed.* **1998**, *37*, 550.
- [3] Y.-L. Loo, R. L. Willett, K. W. Baldwin, J. A. Rogers, *J. Am. Chem. Soc.* **2002**, *124*, 7654.
- [4] J. A. Rogers, K. E. Paul, R. J. Jackman, G. M. Whitesides, *J. Vac. Sci. Tech. B* **1998**, *16*, 59.
- [5] T. W. Odom, J. C. Love, D. B. Wolfe, K. E. Paul, G. M. Whitesides, *Langmuir* **2002**, *18*, 5314.
- [6] Y.-L. Loo, T. Someya, K. W. Baldwin, Z. Bao, P. K. H. Ho, A. Dodabalapur, H. E. Katz, J. A. Rogers, *Proc. Natl. Acad. Sci. USA* **2002**, *99*, 10252.
- [7] T.-W. Lee, J. Zaumseil, Z. Bao, J. W. P. Hsu, J. A. Rogers, *Proc. Natl. Acad. Sci. USA* **2004**, *101*, 429.
- [8] T.-W. Lee, J. Zaumseil, S. H. Kim, J. W. P. Hsu, *Adv. Mater.* **2004**, *16*, 2040.
- [9] J. G. C. Veinot, H. Yan, S. M. Smith, J. Cui, Q. Huang, T. J. Marks, *Nano Lett.* **2002**, *2*, 333.
- [10] E. Menard, L. Bilhaut, J. Zaumseil, J. A. Rogers, *Langmuir* **2004**, *20*, 6871.
- [11] Nonlinearity refers to the changes in absorbance and refractive index as functions of exposure dose. The absorbance of the Shipley photoresist increased upon exposure. See "Microposit S1800 Series Photo Resists" information supplied by the supplier at <http://electronicmaterials.rohmhaas.com>, <http://www.townetech.com/shipley.htm>, and [http://cmi.epfl.ch/materials/Data\\_S1800.pdf](http://cmi.epfl.ch/materials/Data_S1800.pdf), last accessed June 2005.
- [12] M. T. Bernius, M. Inbasekaran, *Adv. Mater.* **2000**, *12*, 1737.
- [13] Y. Koide, M. W. Such, R. Basu, G. Evmenenko, J. Cui, P. Dutta, M. C. Hersam, T. J. Marks, *Langmuir* **2003**, *19*, 86.